MAGNETIC FIELD ANALYSIS OF DC MACHINE BY APPLYING ARTIFICIAL NEURAL NETWORKS TO FINITE ELEMENTS METHOD

K.Nur BEKİROĞLU, İbrahim ŞENOL, Sibel ZORLU, Hülya OBDAN
Yıldız Technical University, Faculty of Electric and Electronics, Department of Electrical Engineering, 80750 Yıldız, Beşiktaş-İstanbul, TÜRKİYE Tel: 902122597070/ Ext. 2555
Fax: 902122594967 E-mail: nbekir@yildiz.edu.tr

***Abstract:** In this study, leakage field of direct current machine is examined by using artificial neural networks in finite element method. Magnetization characteristics of material used in the pole leg is modeled with artificial neural networks. The air gap is optimized as a consequence of field calculation examined nonlinearly with the finite element method. The most appropriate shape of the pole face is determined. Results obtained are compared with the experimental results and proved to be accurate.*

1.INTRODUCTION

As the Cubic spline method, which is preferred for modeling magnetization curves of electrical materials when solving non-linear field problems with finite element method, results in large errors at the points where the curve changes fast, modeling is processed after the curve is divided into several parts at those points. This leads to an increase in modeling costs. Such a disadvantage is dismissed by modeling the curves with artificial neural networks. For learning processes in the artificial neural networks, the back propagation training algorithm is used.

After controlling the leakage field of direct current machine, equipotential points are obtained graphically for working on noload. Appropriate pole face shape is optimized by calculating the flux density across the air gap.

2. MODELLING υ - B^2 CURVES WITH ARTIFICIAL NEURAL NETWORKS

In order to apply Newton-Raphson method on non-linear isotropic problems in solving non-linear problems with finite element method, reluctivity of elements and their slopes with respect to B^2 must be calculated [1].
By using the energy expression,

$$W = B \cdot H \qquad (1)$$

curves $\upsilon = f(B^2)$ are obtained from B-H curves by using the following:

$$W = \upsilon \cdot B^2 \qquad (2)$$

$$B^2 = W / \upsilon \qquad (3)$$

The cubic spline method, one of the exponential function approximation methods for B-H curves, is highly preferred in the application of finite element method to electromagnetic problems. In this paper, the magnetization curve of a DC shunt motor (3.5 kW, 440 V, 9.5 A, 2900 rpm) is modelled with artificial neural networks. Used material is rolled out vertically and has a thickness of 5 mm. B-H curve which represents magnetic flux density varies as a function of magnetic field strength for this DC shunt motor is given in Figure 1.

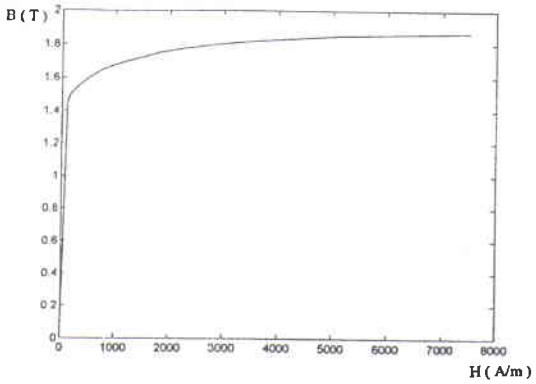

Figure 1. Magnetic flux density variation as a function of magnetic field strength.

When equation (2) is used in equation (1) in order to obtain the reluctivity in terms of H and B,

$$B.H = \upsilon.B^2 \qquad (4)$$

is obtained. After the necessary simplifications, magnetic reluctivity is calculated as:

$$\upsilon = H / B \qquad (5)$$

Reluctivity values is obtained by applying B-H values read from the magnetization curve in Figure 1. By using equation (5), the variation of reluctivity as a function of the square of magnetic flux density is given in Figure 2.

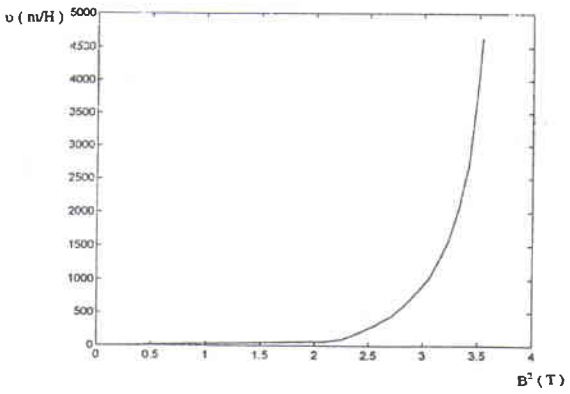

Figure 2. υ-B^2 characteristics obtained by using the magnetization curve in Fig. 1.

The cubic spline method generates large errors at points where the curve varies drastically; therefore modeling operation must be carried out after dividing the curve into several parts at those points. This requirement increases modeling costs. This flaw is corrected by the application of artificial neural networks for modeling the curves. In artificial neural networks method, back-propagation of error algorithm is used for learning operation. [2]

As it is known, back propagation algorithm is used in order to minimize the squared error function between the desired output and actual output of a multi-layer feedforward perceptron. [3]

As there is only one input and one output for artificial neural networks in modeling the curve υ -B^2 , number of nodes in input and output layers is identical and equal to 1. Four nodes are chosen in hidden layer. Network structure for this architecture is presented in Figure 3.

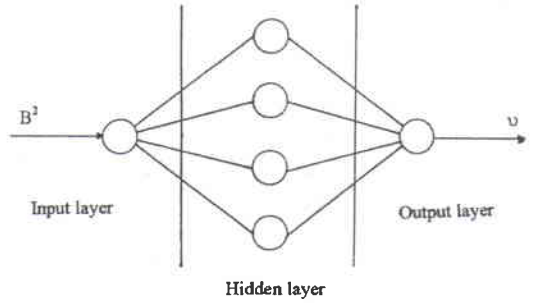

Figure 3. Network architecture used in modeling.

Results of modeling with artificial neural networks has been calculated for different iteration values and learning coefficients. As there is not any linear relationship between iteration and learning, appropriate number of iterations has been investigated and 10,000 iterations have been found to be sufficient. Absolute error is approximately 2% around 10,000 iterations. Curve υ-B^2 as a result of this modeling is presented in Figure 4.

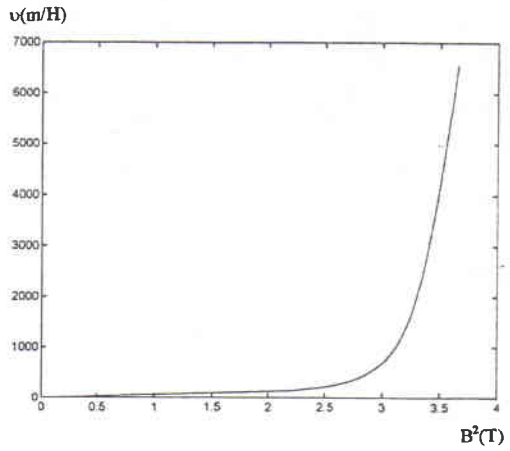

Figure 4. Curve υ-B^2 obtained as a result of modeling with artificial neural networks

3. MAGNETIC FIELD ANALYSIS OF DC MACHINE BY THE APPLICATION OF ARTIFICIAL NEURAL NETWORKS TO THE FINITE ELEMENTS METHOD

Construction diagram of the previously described DC machine is given in Fig. 5.

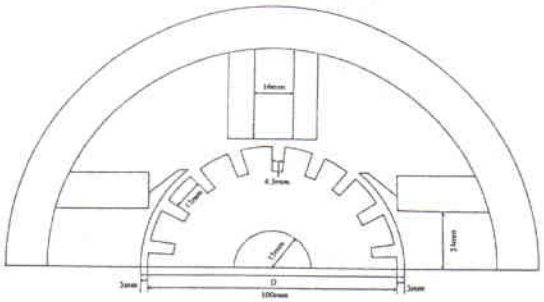

Fig. 5. Construction diagram of the DC machine.

Rotor length l_a is equal to 0.125 m.. Number of turns in a pole is 2600 and the excitation current limits are 0.57 – 3.58 A. In the air gap, for the minimum excitation , it is the case that

$$F=N.I = H.l \qquad (6)$$

where

F: Electromotive force applied to the magnetic circuit
N: Number of turns
I: Current passing through the circuit
l: Width of the air gap.
Then

$$H = \frac{N.I}{l} = \frac{2600x0,57}{3.10^{-3}} = 494000 \ \text{AT/m} = 190 \ \text{A/m}$$

Pole face cross-section is calculated as

$$S = \frac{\pi.D}{2p} l_a = \frac{\pi.106.10^{-3}}{2}.125.10^{-3} = 0.02\text{m}^2$$

[4], where

D: External diameter of the rotor
l_a: Induction length.

Accordingly, air gap reluctance, μ_o being the gap permeability ,

$$\Re = \frac{1}{\mu_o.S} = \frac{3.10^{-3}}{4\pi.10^{-7}.0.02} = 119366 \ \text{H}^{-1}$$

The value of the flux can be obtained as

$$\phi = \frac{2600.0,57}{119366} = 12.10^{-3} \ \text{Wb}$$

and the flux density in the air gap is

$$B = \frac{\phi}{S} = \frac{12.10^{-3}}{0.02} = 0.6 \ \text{T}$$

This is a typical value in DC machine design. Mean flux density to form in the poles for the chosen H value as related to the magnetization characteristics of the material is read as 1,5 T. As this value is around the saturation point of the material, it is appropriate for poles. The actual flux density value in the poles will be calculated by comparing linear and non-linear solutions to the field within the machine with these calculations.

3.1. THE APPLIED FINITE ELEMENTS METHOD

A two-dimensional finite element method is used for the analysis. Accordingly, machine's length in the z-axis is considered infinite. In that case, the magnetic vector potential is only a function of x and y. The general second order differential equation given for the second order limiting value problem, in order to define the field in the DC machine, becomes

$$\frac{\partial}{\partial x}\left(\upsilon\frac{\partial \mathbf{A}}{\partial x}\right)+\frac{\partial}{\partial y}\left(\upsilon\frac{\partial \mathbf{A}}{\partial y}\right)=-\mathbf{J} \qquad (7)$$

where

A: Magnetic vector potential

J: Current density vector

Component z of the magnetic vector potential is equal to zero and current density vector **J** has only z as component; hence the equation (7) becomes

$$\nabla.(\upsilon\nabla.\mathbf{A})=-\mathbf{J} \qquad (8)$$

[5]. When this equation is arranged according to variational formulation, the finite element equation in the matrix form is obtained as

$$\upsilon[K]\{A\}=\{J\} \qquad (9)$$

[6]. Where

K: Coefficients matrix

3.2. INTRODUCTION TO MACHINE GEOMETRY

Physical description of the machine according to the vertical cross-section given in Fig. 5 is presented in Fig. 6.

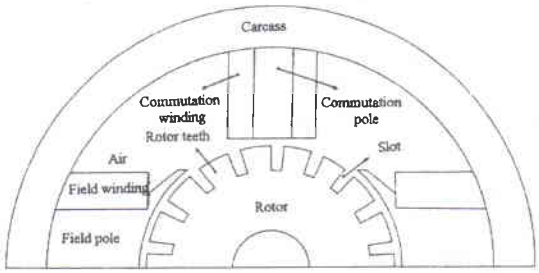

Fig. 6. Physical description of the DC machine

As the machine is symmetrical, only half of the machine will be modeled in the analysis; hence Fig. 6 shows that half. Mathematical model of the machine to be used in the finite element model is presented in Fig. 7.

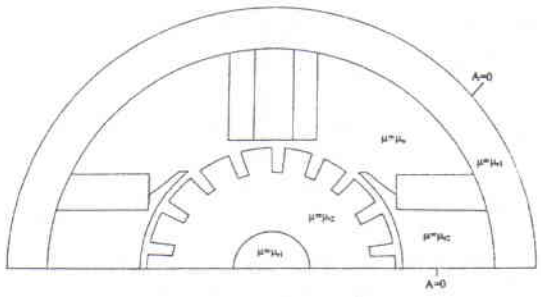

Fig. 7. Mathematical model of the DC machine.

Material for the rotor shaft and carcass is chosen as identical and its relative permeability is picked as 1000. This value is also conserved in the non-linear solution. In the case of linear solution, relative permeability for the pole and rotor iron sheets is picked as 3000 and in non-linear solution, this value is updated for each element.

3.3. FINITE ELEMENTS APPROACH

For the finite element formulation, triangular elements with three nodes are used in the mesh structure. The following are considered in the analysis:

1. The length of the machine on the z -axis is infinite.
2. Displacement currents are ignored .
3. Eddy currents are ignored.
4. Given the linearity of the picked elements, flux density and reluctivity in all points on the triangular elements are considered constant.

As it can be seen in the Fig. 7, magnetic vector potential value is considered to be zero for all boundaries given the DC machine's symmetry. Consequently, homogenous Dirichlet boundary condition is applied for all limits.

3.4. APPLIED MESH STRUCTURE

Mesh structure picked for analysis is presented in Fig. 8. Triangular elements are picked as small as possible in order to improve the solution, as the energy is dense in the air gap. As a stable state analysis is carried out, position of the triangular elements in the air gap is constant. Total number of elements in the mesh is 553 and there are 304 nodes. The element/node ratio is 1.82. This ratio is quite appropriate for a finite element approach. Increasing the total number of elements can improve the results but this also means an increase in the solution duration; hence the above mentioned value is used.

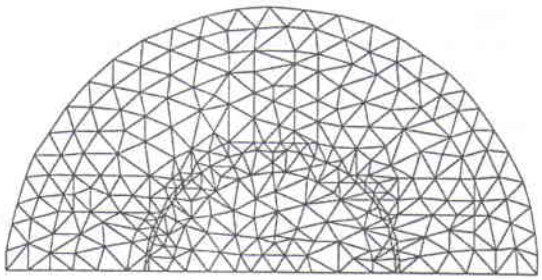

Fig. 8. Mesh structure used in the analysis of the DC machine.

3.5 OBTAINED FIELD DISTRIBUTIONS

In order to evaluate graphically the results obtained with finite element analysis, equipotential points must be plotted on elements. The resulting distribution also gives the flux distribution. Geometry can be redesigned according to the state of leakage fields by inspecting this distribution on the machine. According to the obtained field distributions, it can be deduced that leakage field distributions are minimal. When flux

lines are checked for the slots, it can be seen that these do not influence much the rotor circuit self.

3.6.DISTRIBUTION OBTAINED WITH LINEAR SOLUTION

For the linear solution, the machine is supposed to operate in the linear region. Accordingly, the reluctivity value in the finite element equation is independent of magnetic vector potential. Relative permeability value for our material is picked as 3000; hence the reluctivity value of the iron sheet is picked as 265.25 m/H . In the linear solution, the fact that flux density on the element has various values although the reluctivity value remains constant influences negatively the solution's accuracy. Equipotential lines obtained with the linear solution for a equipotential difference of 0.00055 Wb/m under an excitation current of 0.57 A are presented in Fig.9.

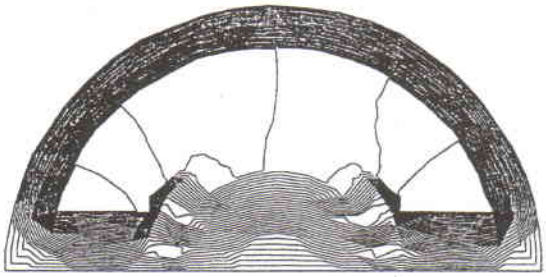

Fig. 9. Equipotential lines obtained with the linear solution.

Air gap flux density values calculated with analytic and finite element method for various excitation currents are presented in Table 1.

Table 1. Flux density values obtained with linear analysis.

Excitation current (A)	Analytic solution B (T)	FEM solution B(T)	Error rate
0.57	0.6	0.53	%11
1.5	1.63	1.43	%12
2.5	2.72	2.21	%18

The fact that the error rate is greater than 10 % points to the shortcomings of the linear solution. As field distributions under other excitation current values are similar, variations are not presented here.

3.7. FIELD DISTRIBUTION OBTAINED WITH THE NON-LINEAR SOLUTION

Field solution for the DC machine is obtained by applying Newton-Raphson method to magnetostatic problems for first order elements [5,7] . Consideration of saturation improves the finite element solution. In the application of Newton-Raphson method, initial values chosen for magnetic vector potentials are the ones obtained with linear solution. Accordingly, number of iterations for Newton-Raphson decreases. Although duration of linear solution may appear as a disadvantage, it is equal to the updating duration in the Newton-Rapson method. In Newton-Rapson method, tolerance is chosen as 10^{-7}.

In non-linear field solution, elements remain linear but for each iteration, reluctivity value on the element is updated. Again, as the elements remain linear, flux density value obtained after each iteration remains the same at all points of the element. Values obtained with non-linear analysis and analytic solution results are presented in Table 2.

Table 2. Flux density values obtained with non-linear analysis

Excitation current (A)	Analytic solution B (T)	FEM solution B(T)	Error rate
0.57	0.6	0.58	%3.3
1.5	1.63	1.57	%3.6
2.5	2.72	2.65	%2.5

Error rate as a result of the non-linear analysis is around 3 %. As saturation is considered, reluctivity values are updated only for material used for poles and rotor iron sheets. For other materials, reluctivity values are accepted as constant and the term $d\upsilon/dB^2$ is accepted as zero. The obtained flux distribution is presented in Fig. 10..

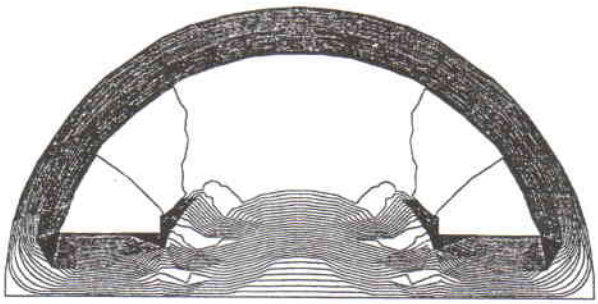

Fig. 10. Flux density obtained with non-linear solution under an excitation current of 2.5 A

υ-B^2 curves of materials used are modeled with artificial neural networks; required reluctivity values for non-linear analysis with finite element are obtained from this method. After the artificial neural networks learn the curve via training, they constitute a weight file. Required reluctivity values are obtained by running the artificial neural networks in test mode. Consequently, after the curve is trained once, it is always ready for further use as the weight file is saved. When solving with finite element is initiated, weight file belonging to the material is determined and required values are read. Artificial neural networks program runs as a subprogram within the finite element method processor program.

4. FIELD DISTRIBUTIONS AND FLUX DENSITIES FOR VARIOUS AIR GAPS AND POLE FACE SHAPES

In this part, field distributions and flux densities for various air gaps and pole face shapes are calculated and compared with analytic solution. Non-linear analysis is used for calculations. Flux density values are calculated by increasing and decreasing the air gap by 1 mm. Results obtained are presented in Table 3 and Table 4.

Table 3. Flux density values for an increase of 1mm in the air gap.

Excitation current(A)	Analytic solution B (T)	FEM solution B(T)	Error rate
0.57	0.46	0.43	%6.5
1.5	1.22	1.19	%2.4
2.5	2.04	1.98	%2.9

Table 4. Flux density values for a decrease of 1mm in the air gap.

Excitation current (A)	Analytic solution B (T)	FEM solution B(T)	Error rate
0.57	0.93	0.85	%8.6
1.5	2.45	2.40	%2.0
2.5	4.08	3.96	%2.9

Pole face shape is then transformed by narrowing at the extremity points of 1.5 mm and widening at central points of 1mm and results obtained from the analysis are presented in Table 5.

Table 5. Flux density values after pole face shape transformation

Excitation current (A)	Analytic solution B (T)	FEM solution B(T)	Error rate
1.5	1.22	1.198	%1.8

As toward the pole extremities the chosen elements get smaller as a result of the given pole shape transformation, a better approximation of results is accomplished. Obtained flux distributions are presented in Fig.11.

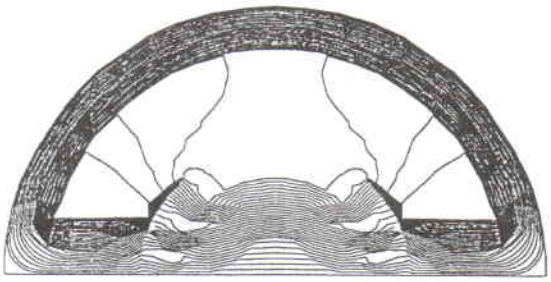

Fig. 11. Flux distribution after pole shape transformation

5.RESULTS

In this present paper, artificial neural networks are used to model material characteristics in non-linear field solution and it is shown that they can be applied in conjunction with finite element method. As artificial neural networks run only in the test phase in the finite element method, solving duration is shortened and the analysis is simplified.

As the interpolation functions of linear three-node elements used in finite element method are first order, the magnetic vector potential is also defined with a first order function. Moreover, increasing the total number of elements in the mesh chosen for finite element method would also increase the solving duration; hence the chosen total number of elements are considered sufficient. The application of non-linear analysis those disadvantages are diminished to a certain degree.

In the analysis of the DC machine, only no-load operation is considered. Load operation analysis is not carried out as the aim is the application of artificial neural networks within finite element method in modeling the magnetization curve.

It is concluded that when flux density values are calculated for various pole face shapes, the flux density value obtained in the air gap by narrowing the air gap at pole extremities and widening it around the center fairly approximates the analytic solution result.

REFERENCES

[1] Silvester, P. P., Cabayan, H. S. and Browne, B., (1973), "Efficient Techniques for Finite-Element Analysis of Electric Machines", IEEE Trans. On PAS, Vol. PAS 92, 1274-1281.

[2] Winrow ve Lehr, M. A., (1990), "Perceptron, Madaline and Back Propagation", Proceedings of the IEEE, Vol.78, No.9, 1417-1439, September.

[3] Lippmann, (1987), "An Introduction to Computing with Neural Nets", IEEE ASSP Magazine, 4-22, April.

[4] Berkol, A.N., (1974), "Elektrik Makinalarının Hesabı", Dizerkonca Matbaası, İstanbul.

[5] Silvester, P.P., Ferrari, R.L., (1996), "Finite Element for Electrical Engineers", 3rd ed., Cambridge University Press, Cambridge.

[6] Chari, M.V.K., Silvester, P.P., (1971), "Finite Element Analysis of Magnetically Saturated DC Machines", IEEE Trans. On PAS., Vol. PAS.90, No.1, 2372-2972, Jan./Feb.

[7] Forghani, B., Lowther, D.A., Silvester, P.P., Stone, G.O., (1983), "Newton-Raphson Finite Element Programs for Axisymmetric Vector Fields", IEEE Trans. On Magnetics, Vol. MAG 19, No.6,2523-2526, November.